Supplementary Information (SI) forNew Journal of Chemistry.
This journal is © The Royal Society of Chemistry 2026

Supplementary Information

Crystallographic, Topological, Antidiabetic, and Docking Evaluation of an Azo-Enamine Ligand and its Triphenyltin(IV) Coordination Polymer

Anisha Das,[a] Debabrata Nama,[a] Chinmoy Majumder,[b] Subhadip Roy,*[c] S. Sureshkumar Singh,[d] Alka Sandham,[d] Salam Pradeep Singh,[e] Manojit Roy,*[a] and Tarun Kumar Misra*[a]

[a]*Department of Chemistry, National Institute of Technology Agartala, Jirania, Tripura (west)-799046, India.* [b]*Department of Chemistry, Indian Institute of Technology, Delhi-110016, India.*

[c]*Department of Chemistry, The ICFAI University Tripura, Kamalghat, Mohanpur, Agartala, 799210, Tripura, India.*

[d]*Department of Botany, School of Life Sciences, Manipur University, Canchipur, Imphal-795003, Manipur, India*

[e]*BRIC - Institute of Bioresources and Sustainable Development, Takyelpat, Imphal West-795001, Manipur, India*

Corresponding authors: **E-mail address*: sroy199@gmail.com (S.R), mroychem@gmail.com (M.R.), tkmisra70@yahoo.com (T.K.M.)

Experimental

Molecular Docking Methodology

Protein Preparation. The three-dimensional (3D) structures of α-glucosidase (PDB ID: 5ZCB) was retrieved from the Protein Data Bank (http://www.rcsb.org/). Protein preparation was done using Protein Preparation Wizard of Molegro Virtual Docker 7.0 (Molexus Software Inc., Denmark). All the water molecules and other non-protein entities were removed, and the hydrogen atoms were added. The protonation states of residues were minimized and optimized. Partial charges were assigned to the protein atoms to ensure accuracy in docking simulations. Additionally, energy minimization was performed on the protein structures to resolve further steric clashes.

Active Site. A deep active-site pocket was composed of domains A, B, and B′. The β→α loop 6 (Phe282–Pro295) included a disordered part (Gly291–Lys294 of the apo-form and Asp289–Glu293 of the complexes) because of poor electron density and showed different conformations between the apo-form and complexes [Reference: W. Auiewiriyanukul, W. Saburi, K. Kato, M. Yao and H. Mori, *FEBS Lett.*, 2018, 592, 2268-2281].

Binding sites and Grid Dimensions. The binding site for α-glucosidase (PDB ID: 5ZCB) was defined within a spherical restriction zone with a radius of 15 Å, centered at grid coordinates X: 1.97, Y: 63.62, Z: 67.26.

Molecular Docking. The compounds were imported into Molegro Virtual Docker (MVD) 7.0 for molecular docking. Both the compounds and protein structures were set for bond flexibility to enable flexible docking simulations. These simulations were conducted to examine binding interactions using a protocol that accounted for side-chain movements within the active site. Molecular docking was performed using the MVD program, which employs a differential evolution algorithm. This method evaluates interaction energy between the ligand and protein, as well as internal interaction energy of the ligand. The PLP (Piecewise Linear Potential) scoring function in MVD was utilized to calculate binding affinities, focusing on van der Waals and hydrogen bond interactions, which are crucial for determining the optimal binding

conformation. The docking engine employed a differential evolution search technique to optimise the spatial orientation and conformation of each compound. The iteration limit was established at 1,500, accompanied with an evolutionary population size of 50. The docking procedure was performed 1,000 times to improve accuracy, producing a minimum of 1,000 postures for each compound. The RMSD threshold for preserving clustered postures was established at 2.00 Å. Each compound was subjected to a minimum of 10 trials to comprehensively explore the conformational space. The optimal posture from each docking session was subsequently chosen for ligand-protein interaction energy analysis.

Binding affinity. The binding affinity of the best docked pose of **H_3L** and ACB was estimated using a multiple linear regression (MLR) equation in Molegro Data Modeller (MVD), which calculates affinity based on various molecular properties such as hydrogen bonds, atom types, solvation energy, and intramolecular interactions.The determination of binding affinity can be used to predict the strength and stability of the interaction between the ligand and the target protein, an important consideration in determining whether it will make a good therapeutic agent.

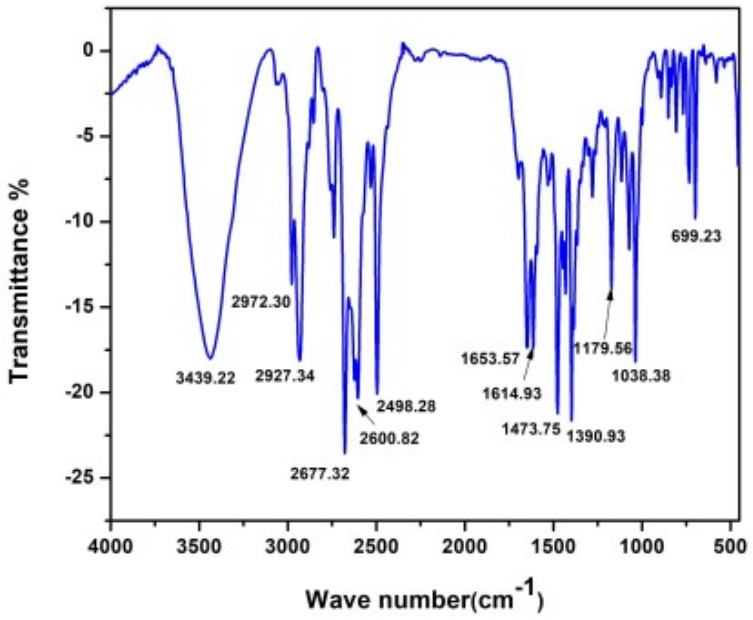

Fig. S1 IR spectrum of triphenyltin(IV) complex, [Ph_3Sn(IV)HL] (**1**)

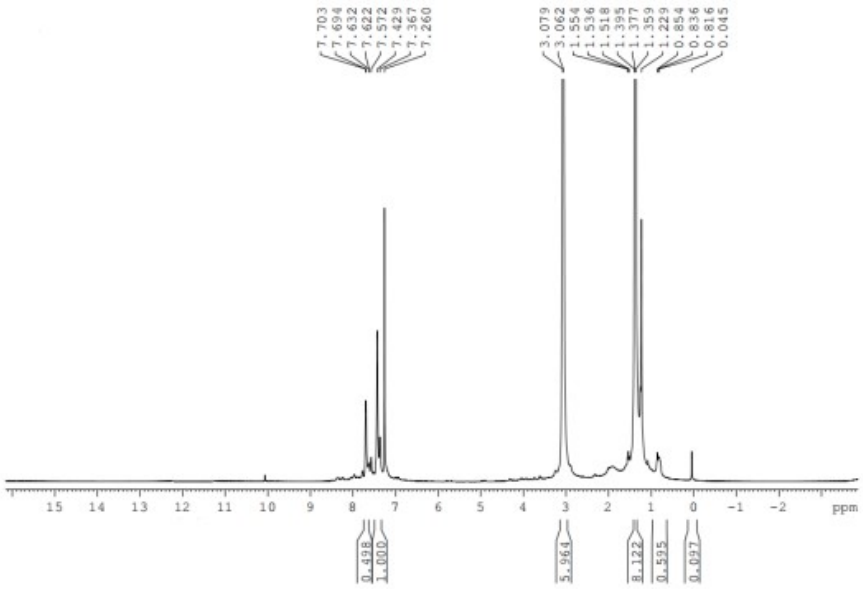

Fig. S2 ^{1}H NMR spectrum of triphenyltin(IV) complex, [Ph_3Sn(IV)HL] (**1**)

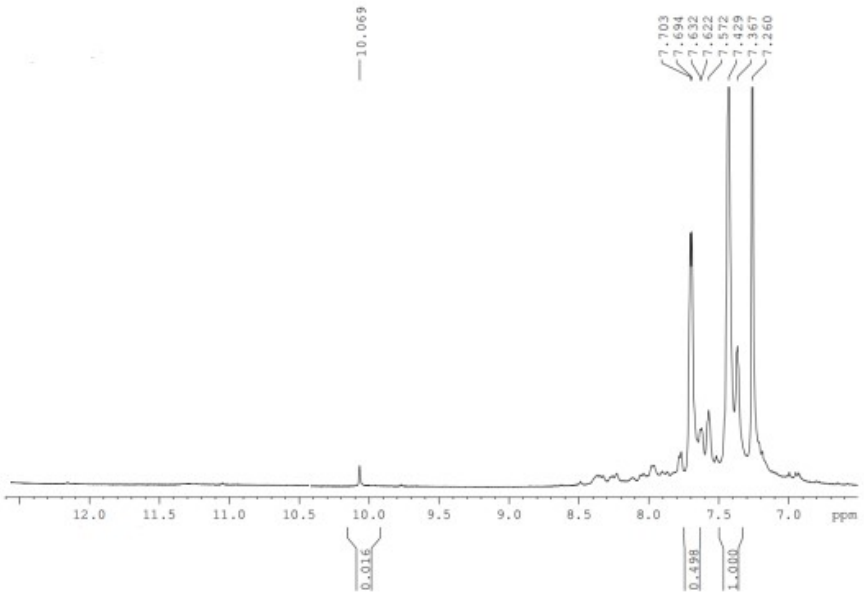

Fig. S3 ^{1}H NMR spectrum of triphenyltin(IV) complex, [Ph_3Sn(IV)HL] (**1**) (Expansion)

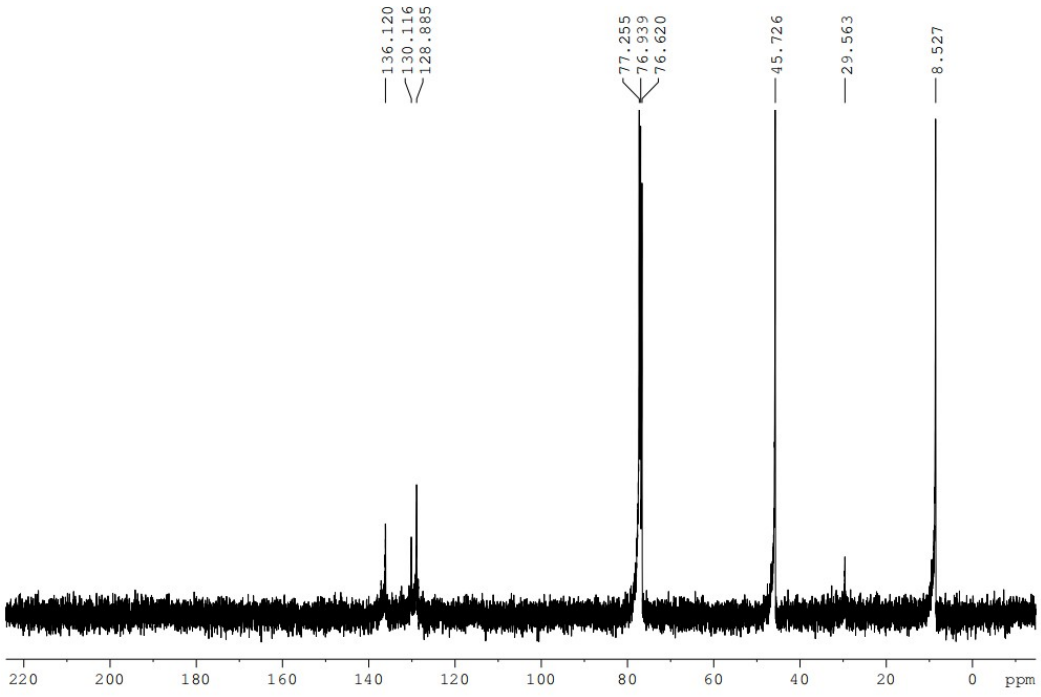

Fig. S4 ^{13}C NMR spectrum of triphenyltin(IV) complex, [Ph_3Sn(IV)HL] (**1**)

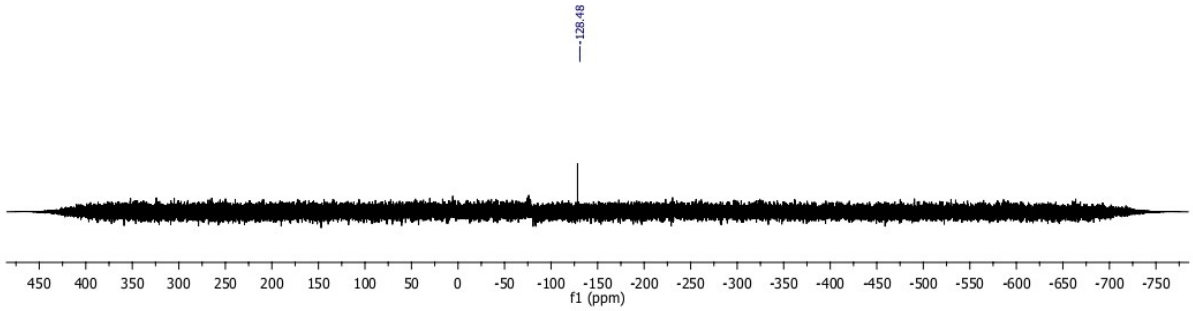

Fig. S5 ^{119}Sn NMR spectrum of triphenyltin(IV) complex, [Ph_3Sn(IV)HL] (**1**)

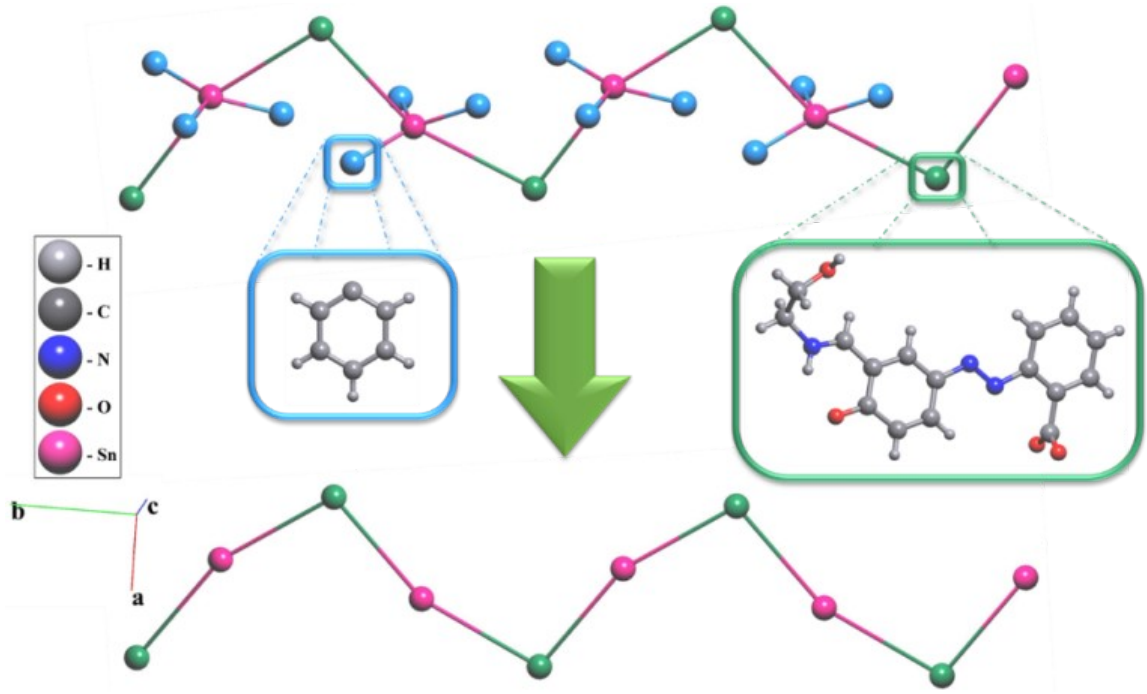

Fig. S6 The underlying net in the standard representation of the valence-bonded MOFs before removing 1-c nodes (top) and after removing 1-c nodes (bottom). Pink spheres correspond to Sn atoms, blue spheres correspond to phenyl ligands, green spheres correspond to **HL** ligands.

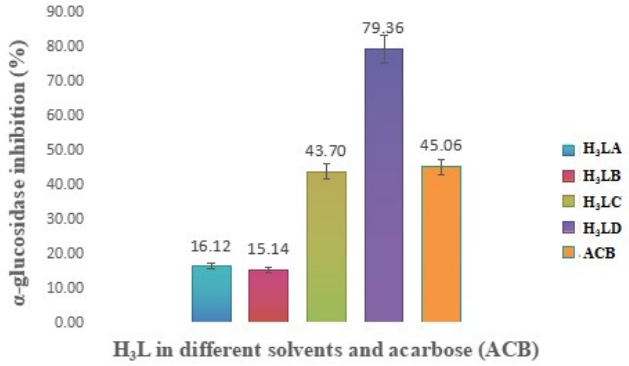

Fig. S7 α-glucosidase inhibition activities of (**H_3L**) in different solvents and acarbose (ACB).

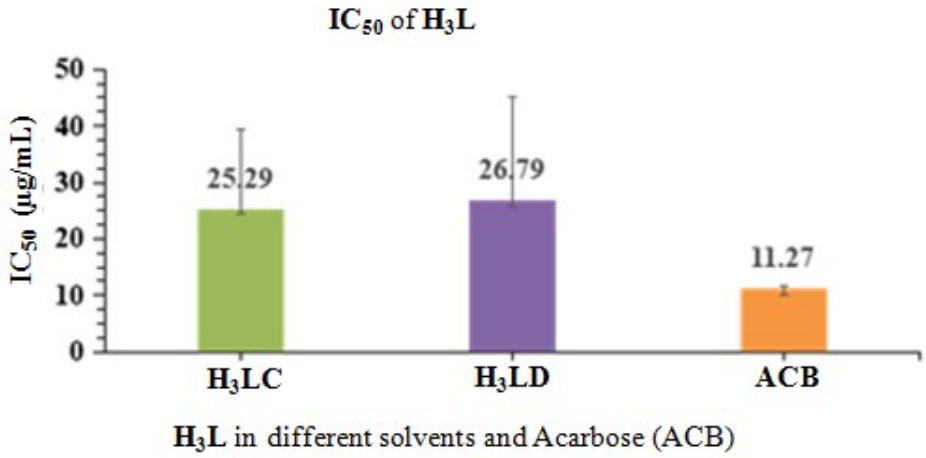

Fig. S8 IC_{50} values of **H_3L** in chloroform and DMSO and acarbose (ACB).

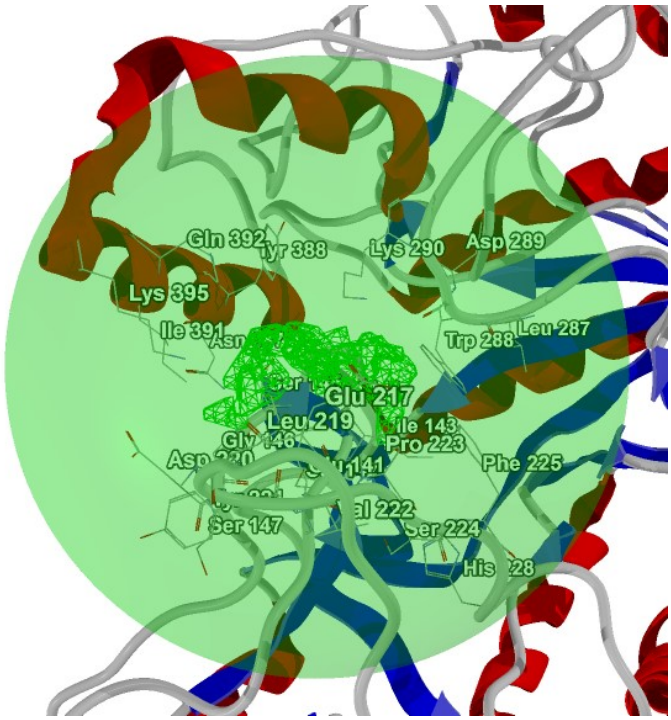

Fig. S9 Binding cavity of 5ZCB (α-glucosidase).

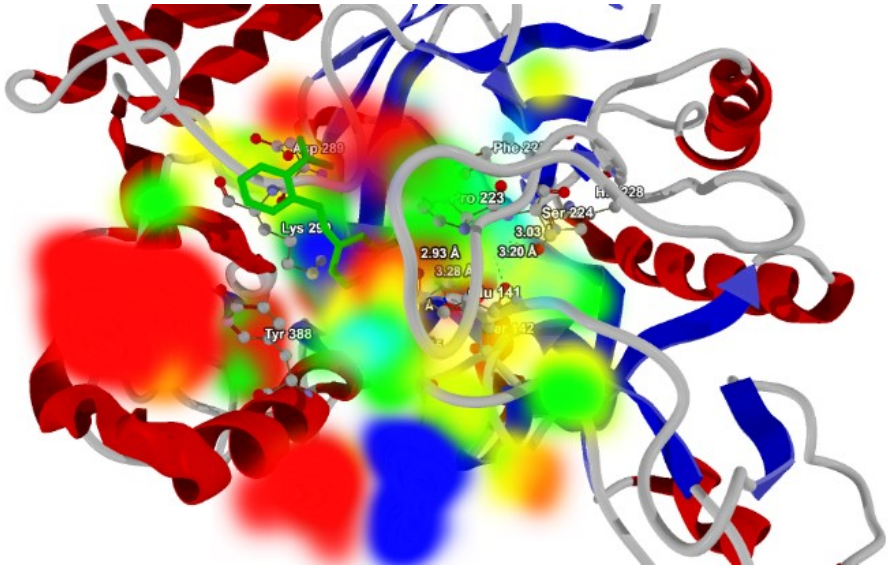

Fig. S10 Energy Map analysis of H_3L (green) at the active site of 5ZCB (α-glucosidase).

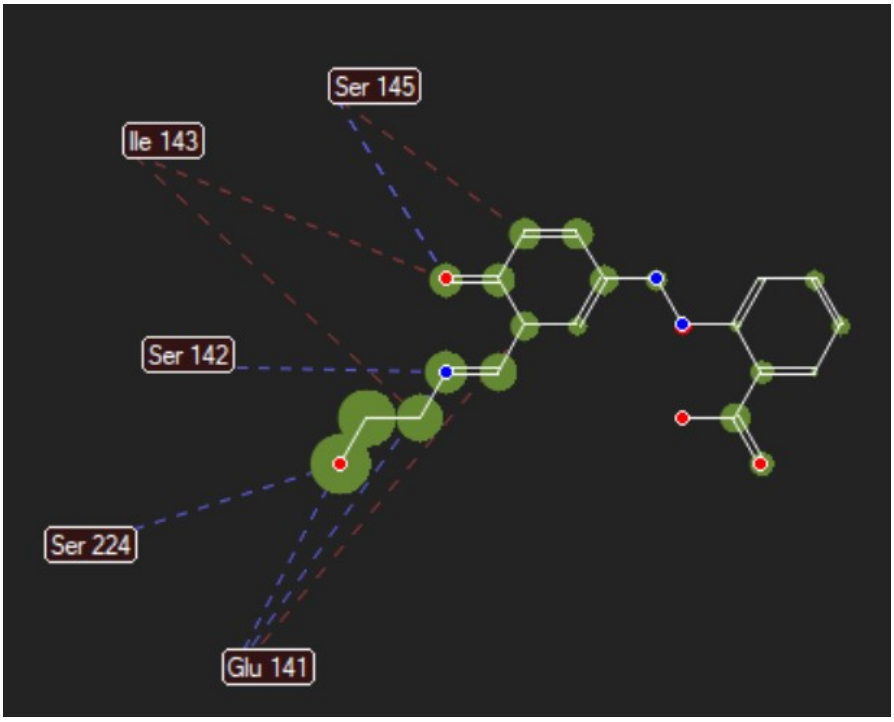

Fig. S11 Molecular interaction analysis of **H_3L** (green) at the active site of 5ZCB (α-glucosidase). No steric interactions were observed.

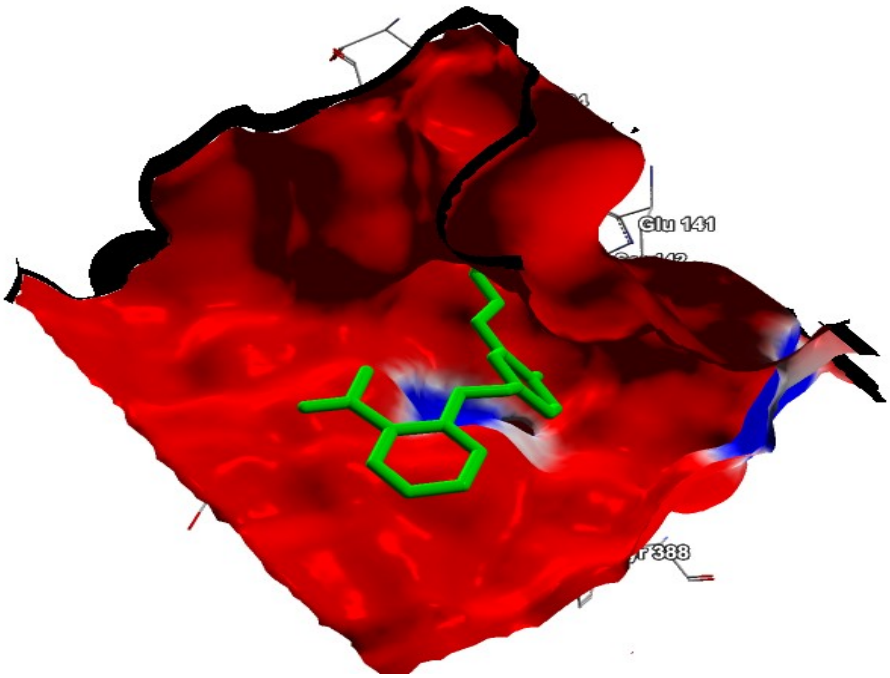

Fig. S12 Electrostatic interaction analysis of **H_3L** (green) at the active site of 5ZCB (α-glucosidase).

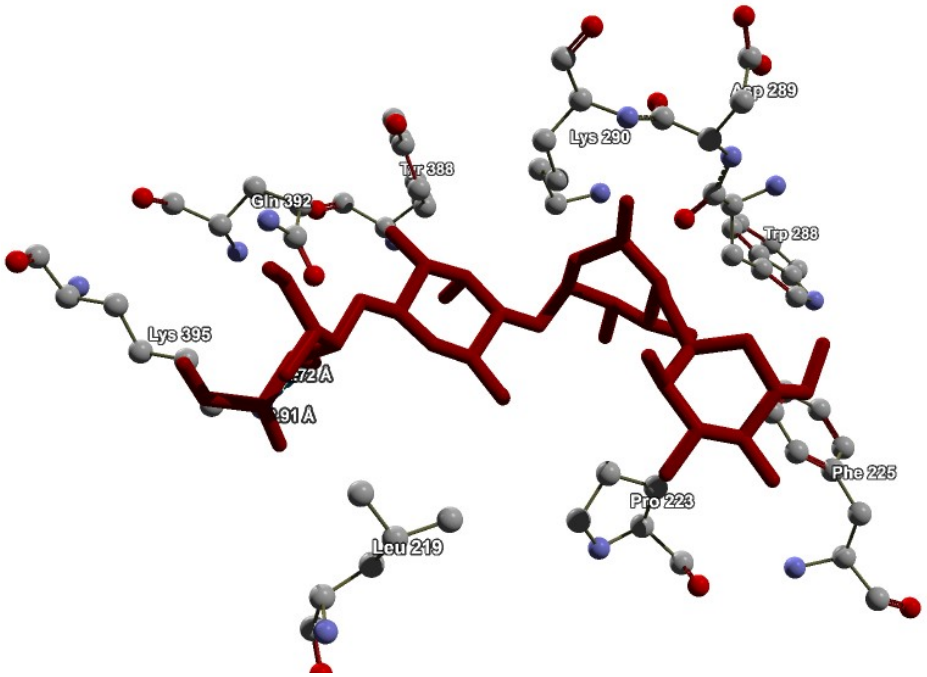

Fig. S13 Molecular interaction of ACB (red) at the active site of 5ZCB (α-glucosidase).

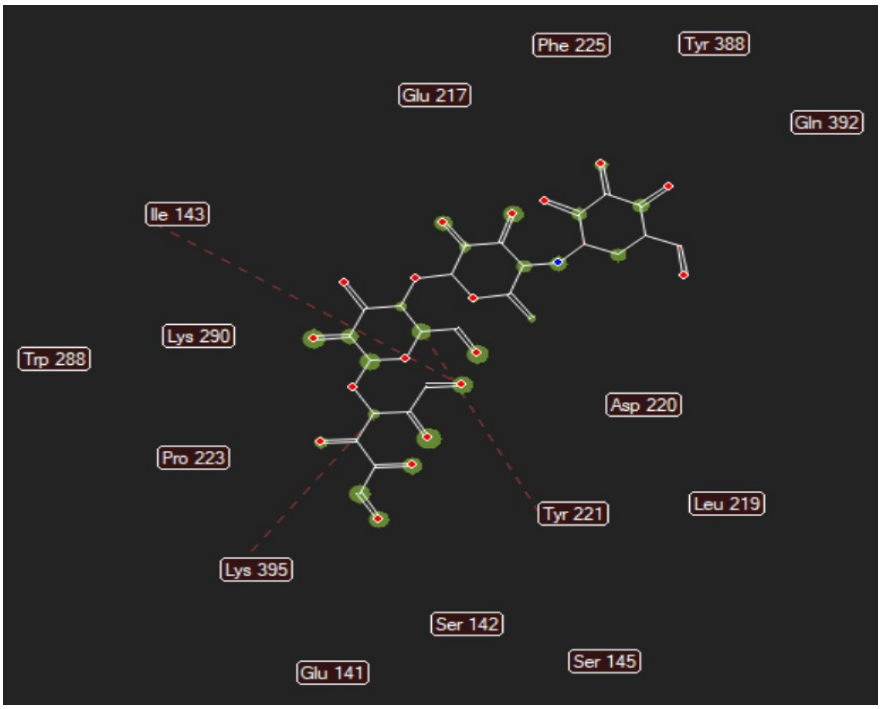

Fig. S14 Molecular interaction analysis of ACB (red) at the active site of 5ZCB (α-glucosidase) showing steric interactions.

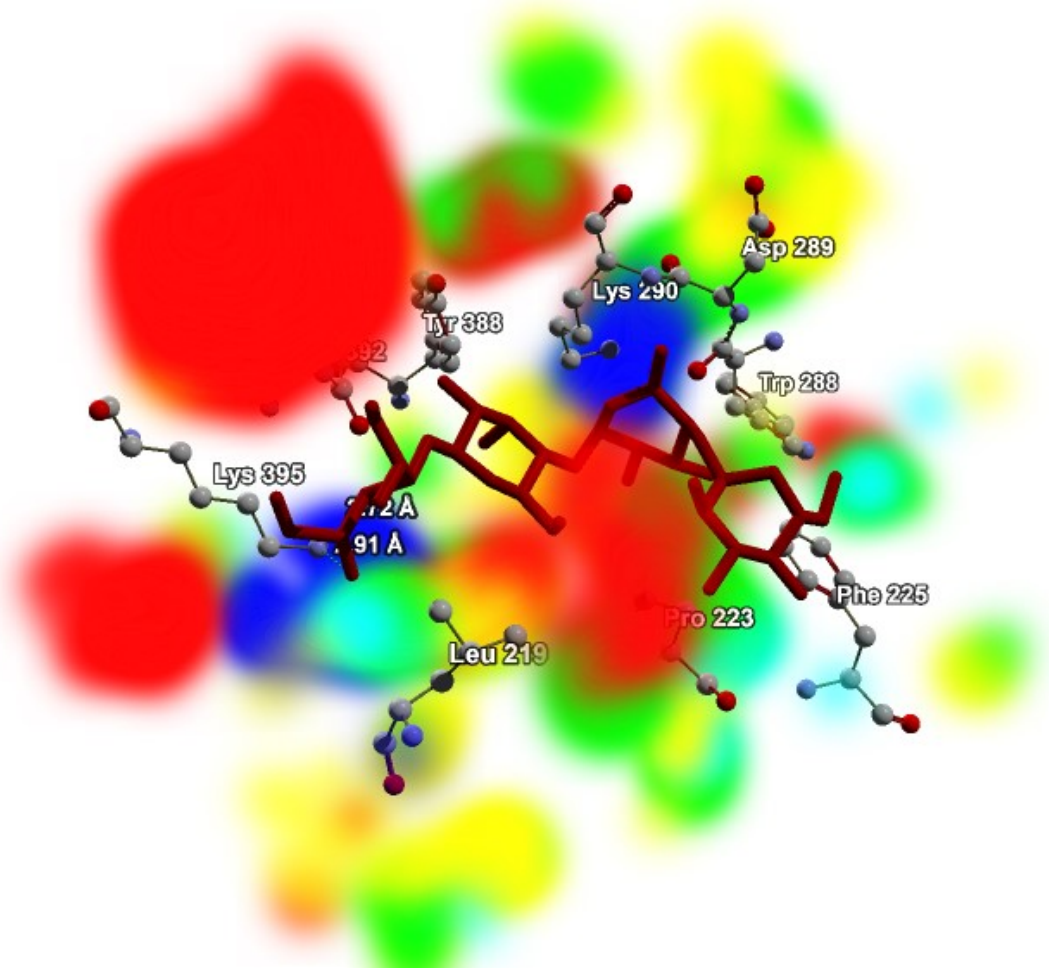

Fig. S15 Energy Map analysis of ACB (red) at the active site of 5ZCB (α-Glucosidase).

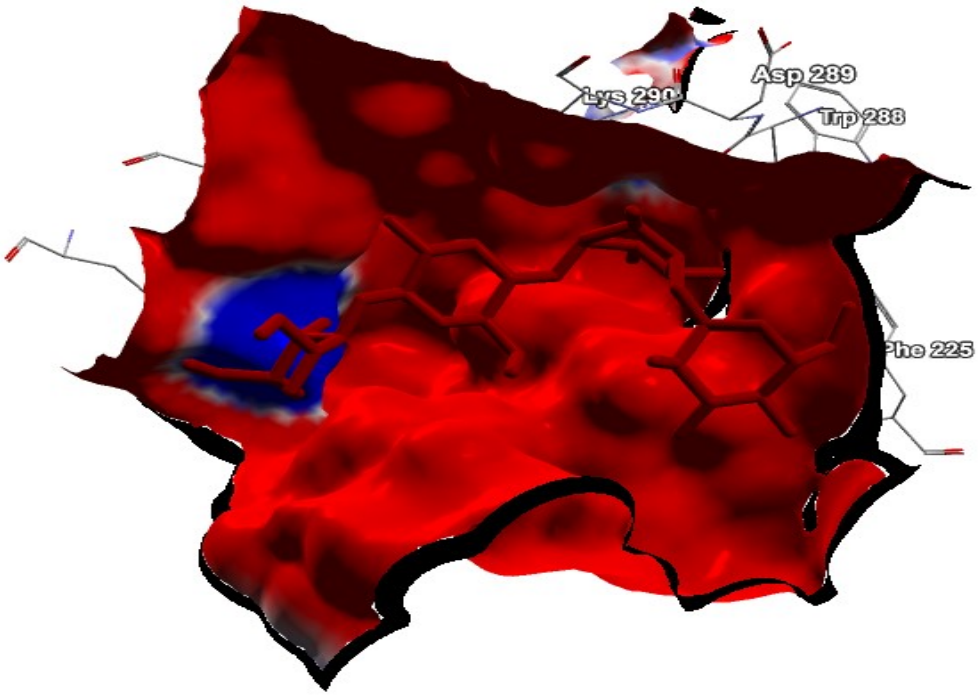

Fig. S16 Electrostatic interaction analysis of ACB (red) at the active site of 5ZCB (α-glucosidase)

Table S1. Overview of crystallographic features and supramolecular synthons in [Ph_3Sn(IV)HL] (**1**) and related Sn(IV) coordination frameworks.

Feature	**[Ph_3Sn(IV)HL] (This Work)**	**Literature Examples**	**References**
Sn(IV) Geometry	Trigonal bipyramidal (5-coordinate), polymeric	Tetrahedral, octahedral, trigonal bipyramidal, square pyramidal	S. M. Abbas, S. Ali, S. T. Hussain and S. Shahzadi, *J. Coord. Chem.*, 2013, **66**, 2217-2234.
Ligand Types	Azo-enamine, carboxylate, phenolic	Carboxylate, dithiocarbamate, hydrazone, thiosemicarbazone, pyridyl, imino etc.	E. R. T. Tiekink, *Appl. Organometal. Chem.*, 1991, **5**, 1-23; J. O. Adeyemi and D. C. Onwudiwe, *Molecules*, 2018, **23**, 2571; B. Taxak, J. Devi, B. Kumar and T. Arora, *BioMetals*, 2024, **37**, 1079-1098;

			B. Blázquez-Tapias, S. Halder, M. A. Mendiola, N. Roy, N. Sahu, C. Sinha, K. Jana and E. López-Torres,. *Chem. Appl.*, 2024, **2024**, 1018375; T. S. Basu Baul, M. R. Addepalli, A. Lyčka, S. van Terwingen and M. Fátima C. Guedes da Silva, *Inorg. Chim. Acta*, 2020, **512**, 119892.
Supramolecular Synthons	N–H···O, O–H···O, π–π stacking	O–H···O, N–H···O, C–H···O, C–H···N, π–π, halogen bonds, stacking, etc.	C. Ma and J. Sun, *Polyhedron*, 2004, **23**, 1547-1555; S. Cheng and J. Yang, *Int. J. Mol. Sci.*, 2023, **24**, 8954; R. P. Bandaru, A. K. Jami and B. K. Tripuramallu, *CrystEngComm*, 2025, **27**, 7081-7093.
Network Topology/Packing Motif	sql (4-c net) layered via H-bond/VDW, polymeric	Monomers, dimers, tetramers, oligomeric ladders, polymeric chains, hexameric drums, macrocycles, clusters, and cages.	T. Tiekink, *Appl. Organomet. Chem.*, 1991, **5**, 1; Debnath, P. Debnath, S. Roy, M.B. Devi, M.M. Devi, K. Sarangthem, S.S. Singh, M.Roy, A.S. Novikov and T.K.Misra, *Inorg. Chim. Acta*, 2024, **559**, 121805; M. Roy, S. Roy, K. S. Singh, J. Kalita, S. S. Singh, *New J. Chem.,* 2016, **40**, 1471; M. Roy, S. Roy, K. S. Singh, J. Kalita

			and S. S. Singh, *Inorg. Chim. Acta*, 2016, **439**, 164; P. Debnath, P. Debnath, M. Roy, L. Sieron, W. Maniukiewicz , T. Aktar, D. Maiti, A.S. Novikov and T. K. Misra, *Crystals*, 2022, **12**, 1582.
Biological Significance	Antidiabetic	Anticancer, antimicrobial, antineoplastic, etc.	D. de Vos, R. Willem, M. Gielen, K. E. Van Wingerden and K. Nooter, *Metal-Based Drugs*, 1998, **5**, 179–188; M. Kemmer, M. Gielen, M. Biesemans, D. de Vos and R. Willem, *Metal-Based Drugs*, 1998, **5**, 189–196; M. Gielen and E. R. T. Tiekink, "^{50}Sn Tin Compounds and Their Therapeutic Potential," in *Metallotherapeutic Drugs and Metal-Based Diagnostic Agents: The Use of Metals in Medicine* (eds. M. Gielen and E.R.T. Tiekink), John Wiley & Sons, Ltd., 2005, ch. 22, pp. 421–439.

Table S2. Docking hits of the compounds at active site

Compound	MolDock Score (kcal/mol)	Rerank Score (kcal/mol)	Interaction(kcal/mol)	H-Bond (kcal/mol)	LE1	LE3	Binding affinity (kcal/mol)
H_3L	–87.92	–79.84	–112.71	–6.86	–3.82	–3.47	–33.0
ACB	–49.41	–54.81	–96.45	–3.07	–1.12	–1.25	–24.04

Table S3. Molecular interaction analysis of **H_3L** and ACB

Compound	Amino Acid---Ligand Interaction	Hybridization	Interaction Energy (kcal/mol)	Interaction Distance
H_3L	Glu141(O)---O(8)	Sp^2---Sp^3	-2.0	3.20 Å
	Ser224(OG)---O(8)	Sp^3---Sp^3	-2.5	3.03 Å
	Glu141(OE1)---N(7)	Sp^2---Sp^2	-0.82	2.93 Å
	Ser142(O)---N(7)	Sp^2---Sp^2	-0.86	3.28 Å
ACB	Lys395(NZ)---O(32)	Sp^3---Sp^2	-2.5	2.72 Å
	Lys395(NZ)---O(36)	Sp^3---Sp^2	-2.5	2.91 Å